JACS
JOURNAL OF THE AMERICAN CHEMICAL SOCIETY
Communication
pubs.acs.org/JACS

Vapor-Phase Metalation by Atomic Layer Deposition in a Metal–Organic Framework

Joseph E. Mondloch,[†,∥] Wojciech Bury,[†,‡,∥] David Fairen-Jimenez,[†,§] Stephanie Kwon,[†] Erica J. DeMarco,[†] Mitchell H. Weston,[†,⊥] Amy A. Sarjeant,[†] SonBinh T. Nguyen,[†] Peter C. Stair,[†] Randall Q. Snurr,[†] Omar K. Farha,*[,†] and Joseph T. Hupp*[,†]

[†]Department of Chemistry, and Chemical and Biological Engineering, Northwestern University, 2145 Sheridan Road, Evanston, Illinois 60208, United States

[‡]Department of Chemistry, Warsaw University of Technology, Noakowskiego 3, 00-664 Warsaw, Poland

Supporting Information

ABSTRACT: Metal–organic frameworks (MOFs) have received attention for a myriad of potential applications including catalysis, gas storage, and gas separation. Coordinatively unsaturated metal ions often enable key functional behavior of these materials. Most commonly, MOFs have been metalated from the condensed phase (i.e., from solution). Here we introduce a new synthetic strategy capable of metallating MOFs from the gas phase: atomic layer deposition (ALD). Key to enabling metalation by **A**LD **I**n **M**OFs (**AIM**) was the synthesis of **NU-1000**, a new, thermally stable, Zr-based MOF with spatially oriented −OH groups and large 1D mesopores and apertures.

Metal–organic frameworks (MOFs) are a class of hybrid materials comprising inorganic nodes and organic linkers.[1−3] In many instances coordinatively unsaturated metal sites (either at the linkers or the nodes) are essential for generating desired functional behavior such as catalysis,[4] gas storage,[5] and gas separation.[6] Most often MOFs have been metal-functionalized from the condensed phase (i.e., solution) either in *de novo* fashion or via postsynthesis modification.[7] Unfortunately, considerable effort is necessary to ensure that excess metals or undesired solvent and other reagents are removed from solution-metalated MOFs. Solvent molecules can also irreversibly ligate otherwise coordinatively unsaturated metal sites, thus yielding less than desirable materials properties.[8] Hence, new synthetic strategies capable of uniformly incorporating open metal sites within MOFs may be attractive for obtaining new functional materials.

Postsynthesis metalation from the vapor-phase could eliminate purification and activation steps and circumvent problems associated with site blocking by solvent molecules. Meilikhov et al. synthesized a variety of metal inclusion compounds (i.e., "metal@MOF" host–guest complexes) by using chemical vapor infiltration from volatile metal complexes under "sublimation-like" conditions. Ideally, this infiltration strategy can lead to high metal@MOF loadings and hybrid materials such as MOFs containing nanoparticles.[9] Unfortunately, there is little control over the spatial distribution of metal species within the MOF and in some instances host–guest interactions may lead to unstable metal@MOFs.

Atomic layer deposition (ALD) is a vapor-phase synthetic technique traditionally used for depositing thin films.[10] The key conceptual advance that ALD embodies over other techniques (e.g., chemical vapor deposition/infiltration) is that precursor molecules deposit only at chemically reactive surface sites, and these reactions are self-limiting. A well-known example makes use of trimethylaluminum ($AlMe_3$) and H_2O to construct thin-films of Al_2O_3, Scheme 1a.[11] Given the sequential and self-limiting nature of ALD, it is uniquely suited for conformal coating of porous materials that exhibit ultrahigh-aspect ratios.[12,13] To date, some striking examples encompass deposition onto micro- and nanopowders[14] and coating of nanoparticle films[15] as well as aerogel networks.[16] ALD is also capable of depositing metal *complexes* if the sequential coreactant (e.g., H_2O) is not used during the deposition. Given the aforementioned capabilities of ALD, we wondered if metalation by **A**LD **I**n a **M**OF (**AIM**, Scheme 1b) could be accomplished; i.e. could MOFs serve as platforms for self-limiting/spatially oriented, interior/surface reaction chemistry?

Scheme 1. Illustration of (a) Thin Film ALD Deposition on a Surface and (b) Metallation by ALD In a MOF (AIM)

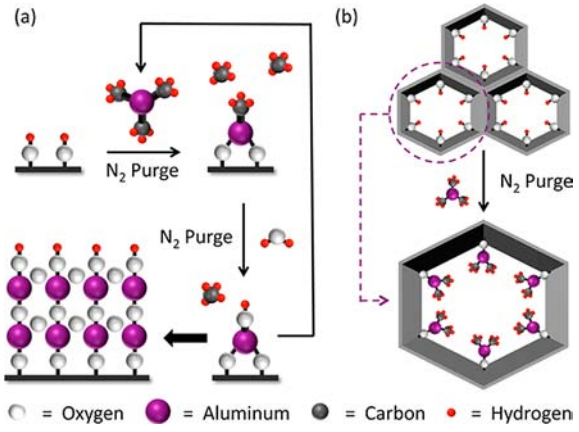

Received: May 22, 2013
Published: July 5, 2013

   dx.doi.org/10.1021/ja4050828 | J. Am. Chem. Soc. 2013, 135, 10294–10297

Three design criteria were considered en route to a MOF broadly suitable for AIM. First, we reasoned that mesoporous (rather than microporous) channels would be necessary to facilitate the diffusion of ALD reactants within the MOF.[13] Recall that diffusion times scale inversely with channel width squared (and directly with channel length squared).[17,18] Second, the desired MOF must be thermally and hydrolytically stable; many ALD reactions are facile between 100−300 °C and employ steam as a coreactant.[11] Finally, spatially oriented functional groups (e.g., −OH groups) must be present for self-limiting metalation reactions to ensue. Given these stringent criteria, we targeted a MOF constructed from hexa-Zr^{IV} nodes[19] and tetratopic linkers.[20,21] Such MOFs are stable to 500 °C,[19] can contain mesoporous channels,[20] and (in principle) can contain spatially oriented −OH groups.[21,22] We describe the synthesis and characterization of a Zr-based MOF (**NU-1000**, *vide infra*) that satisfies all of the aforementioned criteria. We then used **NU-1000** as a platform to demonstrate quantitative, self-limiting metalation by AIM.

Solvothermal reactions of $ZrCl_4$, 1,3,6,8-tetrakis(*p*-benzoic-acid)pyrene (H_4TBAPy),[23,24] and benzoic acid in diethylformamide (DEF) yielded crystals suitable for single-crystal X-ray analysis. The parent-framework node consists of an octahedral Zr_6 cluster capped by eight μ_3-OH ligands. Eight of the twelve octahedral edges are connected to TBAPy units, while the remaining Zr coordination sites (after activation) are occupied by eight terminal −OH ligands.[22] The 3D structure can be described as 2D Kagome sheets linked by TBAPy ligands. Four of the eight terminal −OH groups point into the mesoporous channels, while the remaining terminal hydroxyls lie in smaller apertures between the Kagome sheets. The resultant MOF (Figure 1) has the molecular formula $Zr_6(\mu_3\text{-OH})_8(OH)_8$-

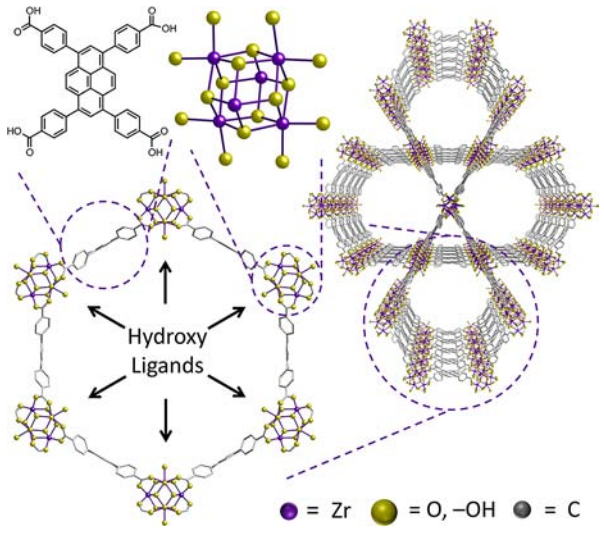

Figure 1. Relevant structural features and representations of **NU-1000**. For simplicity hydrogen atoms are not shown.

$TBAPy)_2$ (**NU-1000**).[25,26] Finally, it was necessary to "activate" **NU-1000** with a HCl/*N*,*N*-dimethylformamide (DMF) mixture in a procedure similar to that of Feng et al.[21] ^{1}H NMR and diffuse reflectance infrared Fourier transform spectroscopies reveal that HCl removes benzoic acid from the Zr_6 nodes, leaving behind terminal −OH groups (SI).

We initiated AIM (*vide infra*) with a microcrystalline powder of **NU-1000**, reasoning that this form would facilitate diffusion of ALD precursors within the MOF. The microcrystalline powder was obtained by switching to DMF as a synthesis solvent. Powder X-ray diffraction (PXRD) patterns of the DEF (simulated)- and DMF-prepared samples are identical, and Pawley refinement of the DMF pattern (SI) shows that the unit cell and symmetry are identical also. In the following, we discuss DMF-prepared samples only.

The N_2 adsorption isotherm of **NU-1000** is best described as type IVc (Figure 3); **NU-1000** has a Brunauer−Emmett−Teller (BET) surface area of 2320 $m^2\ g^{-1}$ and a total pore volume of 1.4 $cm^3\ g^{-1}$. The experimentally measured surface area and total pore volumes are in excellent agreement with the theoretical values of 2280 $m^2\ g^{-1}$ and 1.4 $cm^3\ g^{-1}$ obtained from grand canonical Monte Carlo simulations (GCMC) and subsequent BET analysis (Table S3, SI). DFT-analyzed pore-size distributions indicate pores of diameters at ∼12 Å (consistent with the triangular micropores) and 30 Å (hexagonal mesopores) of **NU-1000**. Thermal gravimetric analysis (TGA) of a sample activated at 120 °C demonstrated that **NU-1000** is stable up to 500 °C. The presence of −OH groups was confirmed by diffuse reflectance infrared Fourier transform spectroscopy (DRIFTS). Sharp peaks appear at wavenumbers 3674 and 3655 cm^{-1} (black curve in Figure 4), which we have assigned to the terminal and bridging −OH stretches of the $Zr_6(\mu_3\text{-OH})_8(OH)_8$ node. These sharp peaks are similar to those measured previously for bridging −OH stretches on the Zr_6 node of UiO-66[27,28] and for bridging and terminal −OH stretches in bulk $Zr(O)(OH)_2$ powders.[29] TGA and temperature-dependent DRIFTS data (SI) are also quantitatively consistent with the assigned −OH content of **NU-1000**. In addition, the temperature-dependent DRIFTS data show that the −OH functionality persists under the conditions of our ALD experiments (*vide infra*).

Microcrystalline samples of **NU-1000** were placed in an ALD reactor at 140 or 110 °C and exposed to diethylzinc ($ZnEt_2$) or $AlMe_3$. The ALD reactions were carried out with the following timing sequence (in seconds): $t_1 - t_2 - t_3$, where t_1 is the precursor pulse time, t_2 the precursor exposure time, and t_3 the N_2 purge time. Metalation was confirmed via inductively coupled plasma-optical emission spectroscopy (ICP-OES). The resultant materials have been termed **Zn-AIM** and **Al-AIM**. On average, we observe 0.5 Zn or 1.4 Al atoms per Zr atom, Table 1. These values correspond to three Zn or eight Al atoms for every Zr_6 node in **NU-1000**. Consistent with ALD-like behavior, longer exposure times (via repeated precursor exposure) did not lead to greater metal loading. To ascertain whether we were fully accessing **NU-1000** under our ALD conditions, we extended exposure times to several hours, rather

Table 1. ICP-OES, BET Surface Areas, and Pore Volumes for NU-1000, Zn-AIM, Al-AIM, Zn-NU-1000, and Al-NU-1000

MOF	metal:Zr	metal:Zr_6	BET surface area ($m^2\ g^{-1}$)	pore volume ($cm^3\ g^{-1}$)
NU-1000	–	–	2320	1.4
Zn-AIM[a]	0.5	3.0	1580	0.9
Al-AIM[b]	1.4	8.1	1160	0.7
Zn-NU-1000	0.6	3.6	1710	1.0
Al-NU-1000	1.7	10.0	1290	0.7

[a] t_1 = 1 s, t_2 = 120 s, t_3 = 120 s. [b] t_1 = 0.015 s, t_2 = 1 s, t_3 = 1 s.

dx.doi.org/10.1021/ja4050828 | J. Am. Chem. Soc. 2013, 135, 10294−10297

than seconds, by immersing samples in solutions containing $ZnEt_2$ or $AlMe_3$ (Table 1, **Zn-NU-1000** and **Al-NU-1000**). The loadings obtained through extended solution-phase exposure are only slightly higher than those from transient ALD.

PXRD measurements (Figure 2) showed that both **Zn-AIM** and **Al-AIM** retain their crystallinity. BET analyses of the N_2

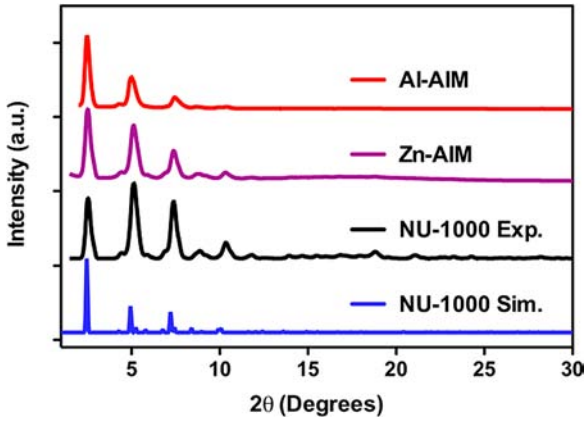

Figure 2. PXRD Patterns of **NU-1000** simulated (Sim.), **NU-1000** experimental (Exp.), **Zn-AIM**, and **Al-AIM**.

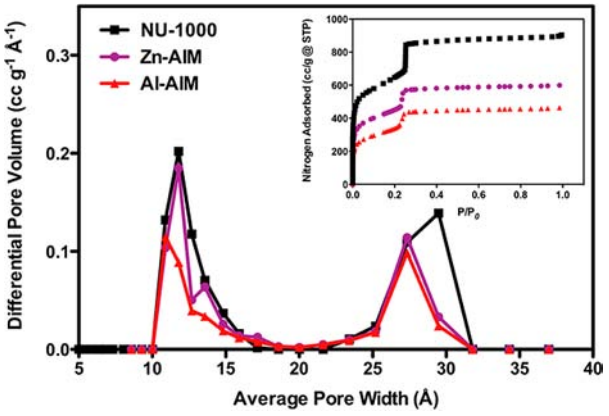

Figure 3. DFT pore size distributions and N_2 adsorption isotherms (inset) for **NU-1000**, **Zn-AIM**, and **Al-AIM**.

adsorption isotherms (Figure 3) indicate a decrease in surface area from 2230 m^2/g for **NU-1000** to 1580 and 1160 m^2/g respectively for **Zn-AIM** and **Al-AIM**. The gravimetric and volumetric (SI) surface areas (along with total pore volumes) decrease with increasing metal loading (Table 1). DFT pore-size distributions (Figure 3), extracted from the N_2 isotherms, indicate that the average diameter of the mesopore shifts from ~30 Å in **NU-1000** to ~27 Å for both **Zn-AIM** and **Al-AIM**.

DRIFTS measurements (Figure 4) confirmed that metalation occurs by reaction with −OH groups. Clearly, the sharp peaks at 3674 and 3655 cm^{-1} have been significantly or completely reduced. For **Zn-AIM**, we speculate that the metalation changes the local symmetry about the Zr_6 cluster, shifting the frequencies of the terminal −OH stretches. Additional studies are in progress to be reported in due course. The DRIFTS data suggest that $ZnEt_2$ is able to react only with −OH groups pointing into the hexagonal channels, while $AlMe_3$ reacts with all terminal −OH groups. (Our findings are reminiscent of the

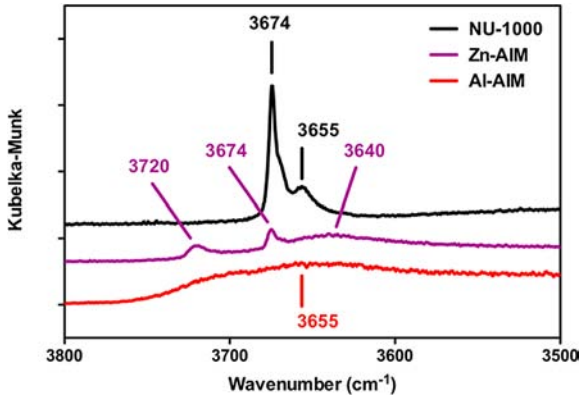

Figure 4. DRIFTS spectra for **NU-1000**, **Zn-AIM**, and **Al-AIM**.

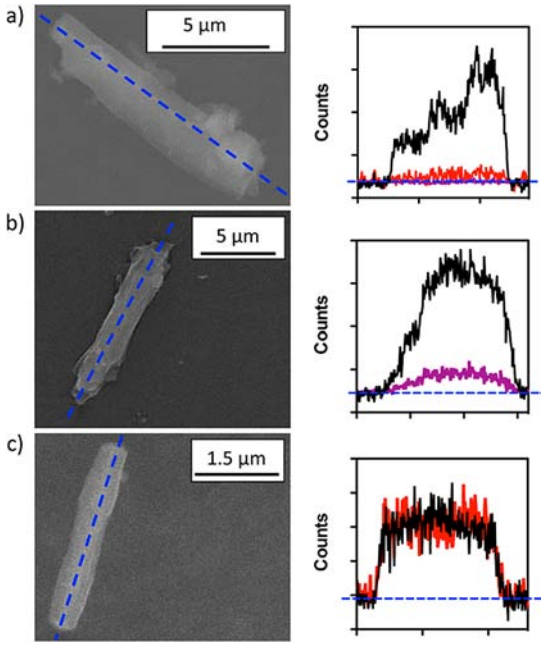

Figure 5. SEM-EDX images and spectra of **NU-1000** (a), **Zn-AIM** (b), and **Al-AIM** (c). EDX scan lines for Zr, Zn, and Al are respectively in black, purple, and red. The dashed blue line indicates where the EDX scan was taken.

observations of Larabi et al. who quantitatively titrated with a solution reagent the −OH ligands on the $Zr_6(O)_4(OH)_4$ node of UiO-67.[28]) To assess Zn and Al incorporation by individual MOF microcrystallites, we turned to scanning electron microscopy−energy dispersive X-ray spectroscopy (SEM-EDX). As shown in Figure 5a, only Zr (black trace) was detected in **NU-1000**; Zn (purple trace) and Al (red line) do not rise above the baseline. The blue line in the image indicates where the EDX scan was performed. When scanning **Zn-** and **Al-AIM** (Figure 5b,c), Zn (purple line) and Al (red line) were detected in the entire **NU-1000** crystal.

As a *proof-of-concept* to show that AIM could be used to elicit new functional behavior we turned to chemical catalysis. The Knoevenagel condensation between ethyl cyanoacetate and benzaldehyde can be catalyzed by Lewis acids, albeit in limited scope and conversion rate.[30] As anticipated, the Zr^{IV} sites in **NU-1000** proved inactive toward the Knoevenagel condensation; however, **Zn-AIM** and **Al-AIM** were active catalysts, which we attribute to the presence of Lewis acidic Al^{III} and Zn^{II}

dx.doi.org/10.1021/ja4050828 | J. Am. Chem. Soc. 2013, 135, 10294−10297

sites in **Zn-** and **Al-AIM**.[31] After catalysis, the solutions were filtered to remove the MOF and were examined by ICP-OES; no Zn or Al was found, consistent with the assignment of **Zn-** and **Al-AIM** as the catalysts. The results demonstrate the potential for ALD to incorporate spatially oriented single-site-like catalytic moieties into ultrahigh-aspect ratio MOFs.

In conclusion, we synthesized and characterized a new Zr-based MOF, **NU-1000**. Given its thermal stability, large 1D pores and apertures, and spatially isolated −OH groups (on the Zr_6 nodes), **NU-1000** is an excellent platform for metalation by AIM and that **Zn-AIM** and **Al-AIM** can be readily synthesized. Based on repetitive precursor/water exposure cycles, initial follow-up studies (to be described in detail when complete) have revealed that AIM (with **NU-1000**) can be used to incorporate (a) multiple other metals, (b) a binary combination of metals, and (c) sizable clusters of metal oxides. We anticipate that AIM will be useful for generating or enhancing MOF chemical competency for a wide variety of applications, including catalysis (demonstrated herein), sorption, and separations.

■ ASSOCIATED CONTENT

Ⓢ Supporting Information

General procedures, materials, and instrumentation; synthesis and characterization of H_4TBAPy, **NU-1000**, **Zn-AIM**, **Al-AIM**, **Zn-NU-1000**, **Al-NU-1000**. This material is available free of charge via the Internet at http://pubs.acs.org.

■ AUTHOR INFORMATION

Corresponding Author

o-farha@northwestern.edu (O.K.F.); j-hupp@northwestern.edu (J.T.H.)

Present Addresses

[§]Department of Chemical Engineering and Biotechnology, University of Cambridge, Pembroke St., Cambridge CB2 3RA, UK.

[⊥]NuMat Technologies, 8025 Lamon Ave., Skokie, IL 60077, United States.

Author Contributions

[‖]J.E.M. and W.B. contributed equally to this work.

Notes

The authors declare no competing financial interest.

■ ACKNOWLEDGMENTS

This research was supported in part by DOE-BES (Grant DE-FG02-08ER15967) and by a DOE EERE Postdoctoral Research Award, EERE Fuel Cell Technologies Program, administered by ORISE for DOE (J.E.M.). ORISE is managed by ORAU under DOE Contract Number DE-AC05-060R23100. We gratefully acknowledge the Foundation for Polish Science through the "Kolumb" Program for financial support. (W.B.). D.F.-J. acknowledges the Royal Society (UK) for a University Research Fellowship. R.Q.S. and P.C.S. acknowledge support from the Chemical Sciences, Geosciences, and Biosciences Division, Office of BES, Office of Science, U.S. DOE Grant DE-FG-02-03ER15457. We thank Dr. Alex Martinson for helpful discussions.

■ REFERENCES

(1) Yaghi, O. M.; O'Keefee, M.; Ockwig, N. W.; Chae, H. K.; Eddaoudi, M.; Kim, J. *Nature* **2003**, *423*, 705.

(2) Férey, G. *Chem. Soc. Rev.* **2007**, *37*, 191.

(3) Horike, S.; Shimomura, S.; Kitagawa, S. *Nat. Chem* **2009**, *1*, 695.

(4) Lee, J.; Farha, O.; Roberts, J.; Scheidt, K.; Nguyen, S. T.; Hupp, J. T. *Chem. Soc. Rev.* **2009**, *38*, 1450.

(5) Dincă, M.; Long, J. R. *Angew. Chem., Int. Ed.* **2008**, *47*, 6766.

(6) Bae, Y.-S.; Lee, C. Y.; Kim, K. C.; Farha, O. K.; Nickias, P.; Hupp, J. T.; Nguyen, S. T.; Snurr, R. Q. *Angew. Chem., Int. Ed.* **2012**, *51*, 1857.

(7) Cohen, S. M. *Chem. Rev.* **2011**, *112*, 970.

(8) Sumida, K.; Stück, D.; Mino, L.; Chai, J.-D.; Bloch, E. D.; Zavorotynska, O.; Murray, L. J.; Dincă, M.; Chavan, S.; Bordiga, S.; Head-Gordon, M.; Long, J. R. *J. Am. Chem. Soc.* **2012**, *135*, 1083.

(9) Meilikhov, M.; Yusenko, K.; Esken, D.; Turner, S.; Van Tendeloo, G.; Fischer, R. A. *Eur. J. Inorg. Chem.* **2010**, 3701.

(10) George, S. M. *Chem. Rev.* **2010**, *110*, 111.

(11) Puurunen, R. L. *J. Appl. Phys.* **2005**, *97*, 1.

(12) Marichy, C.; Bechelany, M.; Pinna, N. *Adv. Mater.* **2012**, *24*, 1017.

(13) Elam, J. W. In *Atomic Layer Deposition of Nanostructured Materials*; Pinna, N., Knez, M., Eds.; Wiley-VCH Verlag & Co.: Weinheim, Germany, 2012; p 227.

(14) Lu, J.; Fu, B.; Kung, M. C.; Xiao, G.; Elam, J. W.; Kung, H. H.; Stair, P. C. *Science* **2012**, *335*, 1205.

(15) Liu, Y.; Gibbs, M.; Perkins, C. L.; Tolentino, J.; Zarghami, M. H.; Bustamante, J.; Law, M. *Nano Lett.* **2011**, *11*, 5349.

(16) Hamann, T. W.; Martinson, A. B. F.; Elam, J. W.; Pellin, M. J.; Hupp, J. T. *Adv. Mater.* **2008**, *20*, 1560.

(17) Gordon, R. G.; Hausmann, D.; Kim, E.; Shepard, J. *Chem. Vap. Deposition* **2003**, *9*, 73.

(18) Elam, J. W.; Routkevitch, D.; Mardilovich, P. P.; George, S. M. *Chem. Mater.* **2003**, *15*, 3507.

(19) Cavka, J. H.; Jakobsen, S.; Olsbye, U.; Guillou, N.; Lamberti, C.; Bordiga, S.; Lillerud, K. P. *J. Am. Chem. Soc.* **2008**, *130*, 13850.

(20) Morris, W.; Volosskiy, B.; Demir, S.; Gándara, F.; McGrier, P. L.; Furukawa, H.; Cascio, D.; Stoddart, F. J.; Yaghi, O. M. *Inorg. Chem.* **2012**, *51*, 6443.

(21) Feng, D.; Gu, Z.-Y.; Li, J.-R.; Jiang, H.-L.; Wei, Z.; Zhou, H.-C. *Angew. Chem., Int. Ed.* **2012**, *51*, 10307.

(22) An alternative formulation of the structure of **NU-1000** would feature oxo and aquo ligands in place of hydroxo ligands. For our purposes, the distinction is not important, as either formulation should be capable of yielding the subsequently observed ALD chemistry.

(23) Stylianou, K. C.; Heck, R.; Chong, S. Y.; Bacsa, J.; Jones, J. T. A.; Khimyak, Y. Z.; Bradshaw, D.; Rosseinsky, M. J. *J. Am. Chem. Soc.* **2010**, *132*, 4119.

(24) Stylianou, K. C.; Rabone, J.; Chong, S. Y.; Heck, R.; Armstrong, J.; Wiper, P. V.; Jelfs, K. E.; Zlatogorsky, S.; Bacsa, J.; McLennan, A. G.; Ireland, C. P.; Khimyak, Y. Z.; Thomas, K. M.; Bradshaw, D.; Rosseinsky, M. J. *J. Am. Chem. Soc.* **2012**, *134*, 20466.

(25) We observe that ∼20−25% of the mesoporous channels contains a secondary structural element (residual electron density plots and N_2 adsorption simulations are given in the SI). We modeled the secondary element as $[Zr_6(\mu_3\text{-}O)_4(\mu_3\text{-}OH)_4]_2(TBAPy)_6$ which connects to 12 Zr_6 nodes of the parent framework through six TBAPy ligands (see SI). Bon et al. also recently detected a secondary element within the pores of a Zr-based MOF.[26] Finally, we cannot rigorously rule out the secondary framework being disordered about the six-fold axis running through the middle of a mesoporous channel.

(26) Bon, V.; Senkovska, I.; Baburin, I. A.; Kaskel, S. *Cryst. Growth Des.* **2013**, *13*, 1231.

(27) Valenzano, L.; Civalleri, B.; Chavan, S.; Bordiga, S.; Nilsen, M. H.; Jakobsen, S.; Lillerud, K. P.; Lamberti, C. *Chem. Mater.* **2011**, *23*, 1700.

(28) Larabi, C.; Quadrelli, E. A. *Eur. J. Inorg. Chem.* **2012**, 3014.

(29) He, M.-Y.; Ekerdt, J. G. *J. Catal.* **1984**, *87*, 381.

(30) Cui, H.-F.; Dong, K.-Y.; Zhang, G.-W.; Wang, L.; Ma, J.-A. *Chem. Commun.* **2007**, 2284.

(31) While AIM, as implemented here, leaves methyl or ethyl ligand(s) on the incorporated metal ions, these are highly reactive and will be removed and released as methane or ethane shortly after exposure to benzaldehyde.